

Performance Evaluation of Adaptive Cooperative NOMA Protocol at Road Junctions

Baha Eddine Youcef Belmekki¹, Abdelkrim Hamza², and Benoît Escrig¹

¹IRIT Laboratory, School of ENSEEIHT, Institut National Polytechnique de Toulouse, France,
e-mail: {bahaeddine.belmekki, benoit.escrig}@enseeiht.fr

²LISIC Laboratory, Electronic and Computer Faculty, USTHB, Algiers, Algeria,
email: ahamza@usthb.dz

Abstract

Vehicular communications (VCs) protocols offer useful contributions in the context of accident prevention thanks to the transmission of alert messages. This is even truer at road intersections since these areas exhibit higher collision risks and accidents rate. On the other hand, non-orthogonal multiple access (NOMA) has been show to be a suitable candidate for five generation (5G) of wireless systems. In this paper, we propose and evaluate the performance of VCs protocol at road intersections, named adaptive cooperative NOMA (ACN) protocol. The transmission occurs between a source and two destinations. The transmission is subject to interference originated from vehicles located on the roads. The positions of the interfering vehicles follow a Poison point process (PPP). First, we calculate the outage probability related to ACN protocol, and closed form expressions are obtained. Then we compare it with other existing protocols in the literature. We show that ACN protocol offers a significant improvement over the existing protocols in terms of outage probability, especially at the intersection. We show that the performance of ACN protocol increases compared to other existing protocols for high data rates. The theoretical results are verified with Monte-Carlo simulations.

Index Terms

NOMA, interference, outage probability, cooperative, vehicular communications, intersections.

I. INTRODUCTION

A. Motivation

Road traffic safety is a major issue, and more particularly at road intersections since there areas are more prone to accidents [1]. In this context, vehicular communications (VCs) protocols

provide several contributions for accident prevention thanks to the sending of alert messages. Such applications require high data rates to enable reliable communications. To increase data rate and spectral efficiency, non-orthogonal multiple access (NOMA) has been shown to be a suitable candidate for the fifth generation (5G) of communication systems as a multiple access scheme [2]. Different from the classical orthogonal multiple access (OMA), NOMA allows multiple users to share the same resource with different power allocation levels. Thus, implementing NOMA in VCs will be beneficial when accidents happen and several vehicles have to send alert messages, or informing other vehicles about the accidents status.

On the other hand, cooperative communications have been shown to increase link reliability of wireless networks using two (or more) communication channels with different characteristics, since each channel undergoes different levels of fading and interference [3]. In this paper, we propose and study the performance of a VCs cooperative NOMA protocol at road junctions.

B. Related Works

The performance of VCs in the presence of interference have been investigated before. Considering highway scenarios, the authors in [4] derive the expressions for the intensity of concurrent transmitters and packet success probability for multilane highway scenarios considering carrier sense multiple access (CSMA) protocols. The authors in [5] analyze the performance of IEEE 802.11p using tools from queuing theory and stochastic geometry. The outage probability is obtained in [6] for Nakagami-m fading and Rayleigh fading channels. Considering intersection scenarios, the authors in [7] compute the success probability in the presence of interference considering a direct transmission road intersection scenario. In [8], the authors calculate the success probability in the presence of interference for intersection scenarios a direct transmission for limited road segments. The performance of vehicle to vehicle (V2V) communications are investigated for multiple intersection streets in [9].

As for NOMA, several works investigate the impact of interference in NOMA networks. The authors in [10] analyze a downlink NOMA network. In [11], the authors analyze a uplink NOMA network. In [12], both uplink and downlink are analyzed. The authors of this the paper investigated the impact of NOMA using direct transmission in [13], cooperative NOMA at intersections in [14], and MRC using NOMA [15], and in millimeter wave vehicular communications in [16], [17]. The authors of this paper also investigated the impact of vehicles mobility, and different transmission schemes on the performance in [18] and [19], [20], respectively.

Regarding cooperative NOMA protocols, The authors in [21] propose a cooperative NOMA protocol in a half duplex mode with a help of a relay. This conventional cooperative NOMA (CCN) protocol [21] improves the performance of the transmission by adding a diversity gain. However, the spectral efficiency of this protocol is reduced due to the use of the half duplex mode. To cope with this limitation, the authors in [22] propose a cooperative protocol, named relaying with NOMA back-haul. In this protocol, the source adjusts the time duration of the transmission based on the global instantaneous channel state information (CSI). However, global instantaneous CSI at the source can be hard to obtain in practice, especially for real time scenarios such as road safety scenarios. Following this line of research, we propose an adaptive cooperative NOMA (ACN) protocol at road junctions for VCs in the presence of interference.

C. Contributions

The contributions of this paper are as follows:

- We propose and evaluate the performance of VCs protocol at at road intersections in the presence of interference.
- We calculate the outage probability related to ACN protocol, and closed form expressions are obtained considering a scenario involving a source, and two destinations.
- We compare the performance of ACN protocol with other existing protocols in the literature. We show that ACN protocol offers a significant improvement in terms of outage probability, especially at intersections.
- We show that the performance of ACN protocol increases compared to other existing protocols for high data rates.
- All results and the theoretical analysis are verified with Monte Carlo simulations.

II. SYSTEM MODEL

In this paper, we consider a NOMA transmission between a source S , and two destinations, denoted D_1 and D_2 . The triplet $\{S, D_1, D_2\}$ denotes the nodes and their locations as depicted in Fig.1. We consider an intersection scenario involving two perpendicular roads, an horizontal road denoted by X , and a vertical road denoted by Y . In this paper, we consider both V2V and vehicle-to-infrastructure (V2I) communications¹, therefore, any node of the triplet $\{S, D_1, D_2\}$

¹The Doppler shift and time-varying effect of V2V and V2I channel are beyond the scope of this paper.

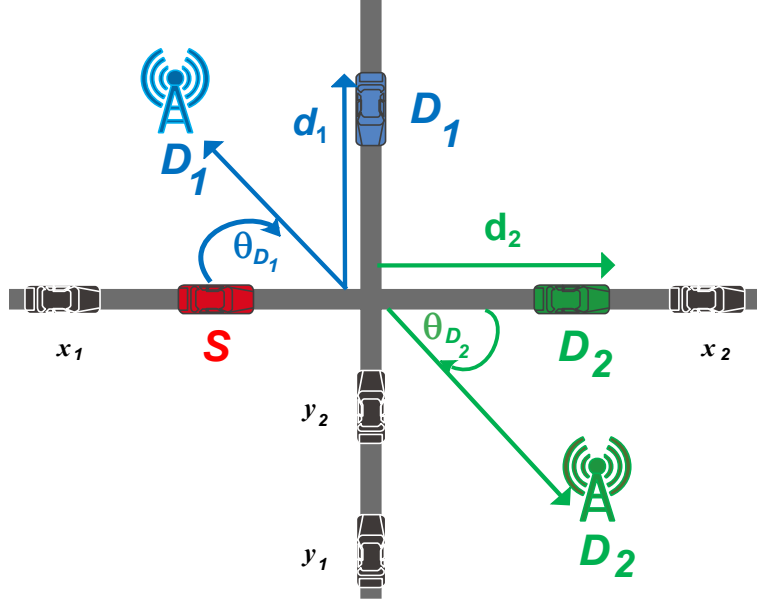


Fig. 1: NOMA system model for VCs. The nodes D_1 and D_2 can be vehicles or as part of the communication infrastructure.

can be either on the road or outside the road. We denote by d_i and θ_i , the distance between the node D_i and the intersection, and the angle between the node D_i and the X road, where $i \in \{1, 2\}$ as shown in Fig.1.

The transmission is subject to interference that is originated from vehicles located on the roads. The set of interfering vehicles located on the X road, denoted by Φ_X (resp. on the Y road, denoted by Φ_Y) are modeled as a one-dimensional homogeneous Poisson point process (1D-HPPP), i.e., $\Phi_X \sim 1D\text{-HPPP}(\lambda_X, x)$ (resp. $\Phi_Y \sim 1D\text{-HPPP}(\lambda_Y, y)$), where x and λ_X (resp. y and λ_Y) are the position of interfering vehicles and their intensity on the X road (resp. Y road). The notation x and y denotes both the interfering vehicles and their locations. The transmission is subject to path loss between the nodes a and b , termed as l_{ab} , where $l_{ab} = \|a - b\|^{-\alpha}$, and α is the path loss exponent. We consider a slotted ALOHA protocol with parameter p , i.e., every node can access the medium with a probability p [23].

Several works in NOMA order the receiving nodes by their channel states [2], [21]. However, we consider that the receiving nodes are ordered according to their quality of service (QoS) priorities, since it has been show that it is more realistic assumption [24], [25]. We consider a scenario in which D_1 needs low data rate but has to be served immediately, whereas D_2 requires high data rate but can be served later. For instance, D_1 can be a vehicle that needs to receive

safety data information about an accident in its surrounding, whereas D_2 can be a user that accesses an internet connection. We also consider an interference limited scenario, and thus, we set the power of the additive noise to zero. We assume, without loss of generality, that all nodes transmit with a unit power. The signal transmitted by S , denoted χ_S , is a mixture of the message intended to D_1 and D_2 . This can be expressed as

$$\chi_S = \sqrt{a_1}\chi_{D_1} + \sqrt{a_2}\chi_{D_2},$$

where a_i is the power coefficients allocated to D_i , and χ_{D_i} is the message intended to D_i . Since D_1 has a higher power allocation than D_2 , that is, $a_1 \geq a_2$, then D_1 comes first in the decoding order. Note that, $a_1 + a_2 = 1$.

The signal received at D_i is then expressed as

$$\mathcal{Y}_{D_i} = h_{SD_i}\sqrt{l_{SD_i}}\chi_S + \sum_{x \in \Phi_{X_{D_i}}} h_{D_i,x}\sqrt{l_{D_i,x}}\chi_x + \sum_{y \in \Phi_{Y_{D_i}}} h_{D_i,y}\sqrt{l_{D_i,y}}\chi_y,$$

where \mathcal{Y}_{D_i} is the signal received by D_i . The messages transmitted by the interfering node x and y , are denoted respectively by χ_x and χ_y , h_{ab} denotes the fading coefficient between node a and b , and it is modeled as $C\mathcal{N}(0, 1)$. The power fading coefficient between the node a and b , denoted $|h_{ab}|^2$, follows an exponential distribution with unit mean. The aggregate interference is defined as

$$I_{X_{D_i}} = \sum_{x \in \Phi_{X_{D_i}}} |h_{D_i,x}|^2 l_{D_i,x}, \quad (1)$$

$$I_{Y_{D_i}} = \sum_{y \in \Phi_{Y_{D_i}}} |h_{D_i,y}|^2 l_{D_i,y}, \quad (2)$$

where $I_{X_{D_i}}$ denotes the aggregate interference from the X road at D_i , $I_{Y_{D_i}}$ denotes the aggregate interference from the Y road at D_i , $\Phi_{X_{D_i}}$ denotes the set of the interferers from the X road at D_i , and $\Phi_{Y_{D_i}}$ denotes the set of the interferers from the Y road at D_i .

III. ACN PROTOCOL

First, we consider the scenario in which D_1 acts as relay to transmit the message to D_2 ². At the beginning of each transmission, S sends the superimposed signal to D_1 and D_2 using a direct transmission [26]. If D_2 decodes its desired message, it sends a 1-bit positive acknowledgement (ACK) to S and D_1 , and thus, the transmission occurs in one phase. However, if D_2 is unable to

²The relay selection algorithms are out of the scope of this paper.

decode its desired message, it sends a 1-bit negative acknowledge (NACK) to S and D_1 . Hence, if D_1 decodes its desired message and D_2 message, it sends D_2 message using cooperative transmission [3] using OMA. Thus, the transmission occurs in two phases.

Now, we consider the scenario in which D_2 acts as relay to transmit the message to D_1 . In this same way, S sends the superimposed message to D_1 and D_2 using a direct transmission. If D_1 decodes its desired message, it sends a 1-bit ACK to S and D_2 , and thus, the transmission occurs in one phase. However, if D_1 is unable to decode its desired message, it sends a 1-bit NACK to S and D_1 . Hence, if D_2 decodes D_1 message, it sends D_1 message using cooperative transmission, and without using NOMA. Thus, the transmission occurs in two phases³. The flow charts of ACN protocol related to D_1 and D_2 are respectively given by Fig.2 and Fig.3. The ACN protocol switches to cooperative transmission only if the direct transmission is not feasible. This will induce a latency because the transmission will occur during two time slots instead of one time slot. However, as we will show in Section V, the ACN protocol increases the performance in terms of outage probability compared to other transmission schemes and protocols in the literature.

IV. ACN PROTOCOL OUTAGE EXPRESSIONS

A. Signal-to-Interference Ratio (SIR) Expressions

The outage probability is defined as the probability that the signal-to-interference ratio (SIR) at the receiver node is below a given threshold. According to successive interference cancellation (SIC) [27], D_1 will be decoded first since it has the higher power allocation, and D_2 message will be considered as interference. The SIR at D_1 to decode its desired message, denoted $\text{SIR}_{D_{1-1}}$, is expressed as

$$\text{SIR}_{D_{1-1}} = \frac{|h_{SD_1}|^2 l_{SD_1} a_1}{|h_{SD_1}|^2 l_{SD_1} a_2 + I_{X_{D_1}} + I_{Y_{D_1}}}. \quad (3)$$

Similarly, The SIR at D_1 to decode D_2 message, denoted $\text{SIR}_{D_{1-2}}$, is expressed as⁴

$$\text{SIR}_{D_{1-2}} = \frac{|h_{SD_1}|^2 l_{SD_1} a_2}{I_{X_{D_1}} + I_{Y_{D_1}}}. \quad (4)$$

³Note that ACN protocol does not need to perform channel estimation to switch between direct transmission and cooperative transmission.

⁴Perfect SIC is considered in this work, that is, no fraction of power remains after SIC process.

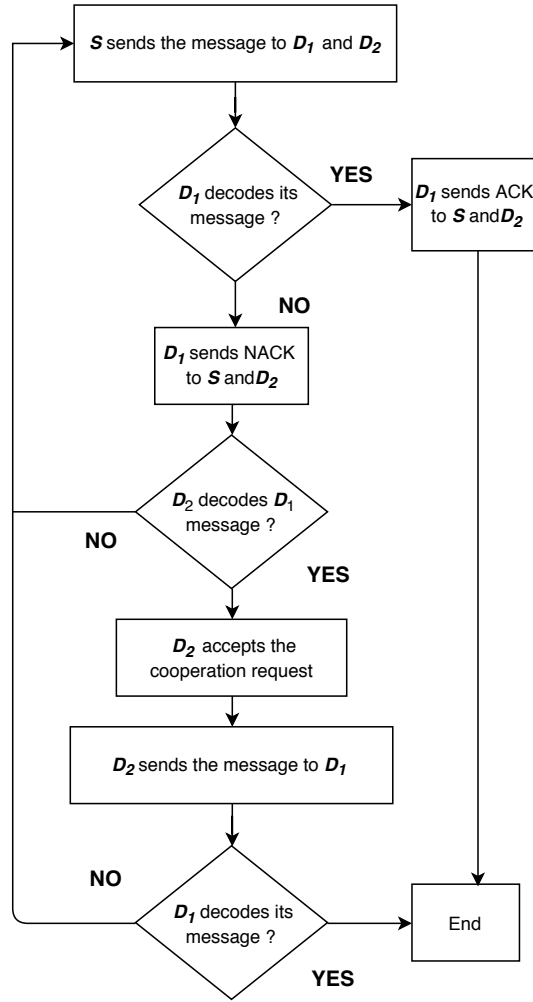


Fig. 2: Flow chart of ACN protocol at D_1 .

Since D_2 has the lower power allocation, it decodes D_1 message first, then decodes its intended message. The SIR at D_2 to decode D_1 message, denoted $\text{SIR}_{D_{2-1}}$, is expressed as

$$\text{SIR}_{D_{2-1}} = \frac{|h_{SD_2}|^2 l_{SD_2} a_1}{|h_{SD_2}|^2 l_{SD_2} a_2 + I_{X_{D_2}} + I_{Y_{D_2}}}. \quad (5)$$

The SIR at D_2 to decode its desired message, denoted $\text{SIR}_{D_{2-2}}$, is expressed as

$$\text{SIR}_{D_{2-2}} = \frac{|h_{SD_2}|^2 l_{SD_2} a_2}{I_{X_{D_2}} + I_{Y_{D_2}}}. \quad (6)$$

When using the cooperative transmission, the node that acts as a relay uses OMA instead of NOMA, since the transmission involves only one receiving node. Hence, the SIR at the receiver

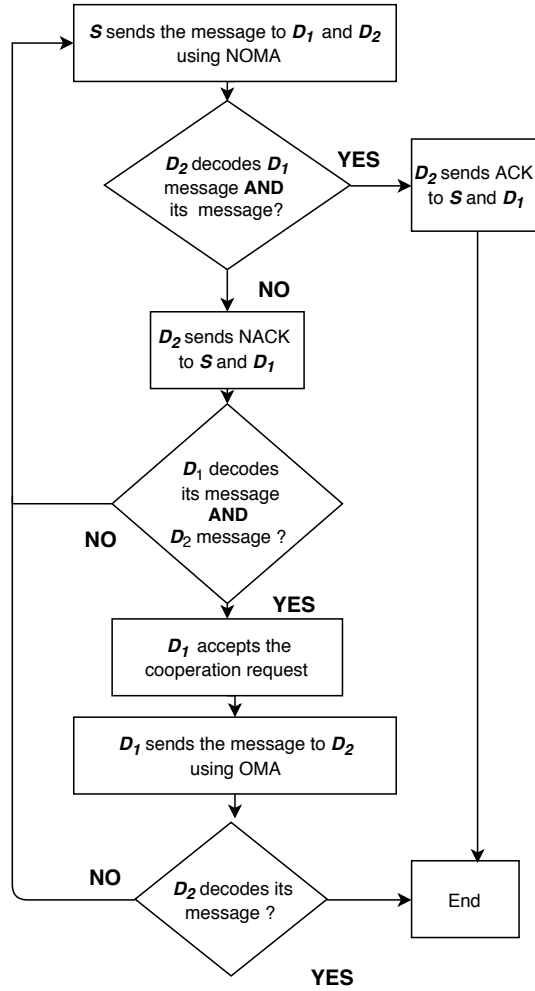


Fig. 3: Flow chart of ACN protocol at D_2 .

is then expressed as

$$\text{SIR}_{D_k D_l}^{(\text{OMA})} = \frac{|h_{D_k D_l}|^2 l_{D_k D_l}}{I_{X_{D_l}} + I_{Y_{D_l}}}, \quad (7)$$

where $\{k, l\} \in \{1, 2\}$.

B. ACN Outage Event Expressions

Now, we will express the outage events related to the ACN protocol for D_1 and D_2 . The outage events related to D_1 and D_2 using ACN protocol, denoted respectively by $\mathcal{O}_{\text{ACN}}(D_1)$ and $\mathcal{O}_{\text{ACN}}(D_2)$, can be expressed as

$$\mathcal{O}_{\text{ACN}}(D_1) = 1 - \mathcal{O}_{\text{ACN}}^{\text{C}}(D_1), \quad (8)$$

and

$$\mathcal{O}_{\text{ACN}}(D_2) = 1 - \mathcal{O}_{\text{ACN}}^C(D_2), \quad (9)$$

where $\mathcal{O}_{\text{ACN}}(D_1)$ and $\mathcal{O}_{\text{ACN}}(D_2)$ denote respectively the success events related to D_1 and D_2 . The expression of $\mathcal{O}_{\text{ACN}}^C(D_1)$ and $\mathcal{O}_{\text{ACN}}^C(D_2)$ are respectively given by

$$\mathcal{O}_{\text{ACN}}^C(D_1) = \{\text{DT}_{SD_1}^C\} \cup \{\text{DT}_{SD_1} \cap \text{RT}_{S,D_2,D_1}^C\}, \quad (10)$$

and

$$\mathcal{O}_{\text{ACN}}^C(D_2) = \{\text{DT}_{SD_2}^C\} \cup \{\text{DT}_{SD_2} \cap \text{RT}_{S,D_1,D_2}^C\}, \quad (11)$$

where $\text{DT}_{SD_n}^C$, RT_{S,D_2,D_1}^C , and RT_{S,D_1,D_2}^C are expressed as

$$\text{DT}_{SD_n}^C = \bigcap_{i=1}^n \text{SIR}_{SD_{n-i}} < \Theta_i^{(1)}, \quad (12)$$

and

$$\text{RT}_{S,D_2,D_1}^C = \left\{ \text{SIR}_{SD_{2-1}} \geq \Theta_1^{(2)} \cap \text{SIR}_{D_2D_1}^{(\text{OMA})} \geq \Theta_1^{(2)} \right\}, \quad (13)$$

and

$$\text{RT}_{S,D_1,D_2}^C = \left\{ \bigcap_{i=1}^2 \text{SIR}_{SD_{1-i}} \geq \Theta_i^{(2)} \cap \text{SIR}_{D_1D_2}^{(\text{OMA})} \geq \Theta_2^{(2)} \right\}. \quad (14)$$

The decoding threshold $\Theta_i^{(n)}$ is defined as

$$\Theta_i^{(n)} \triangleq 2^{n\mathcal{R}_i} - 1, \quad (15)$$

where \mathcal{R}_i is the target data rate of D_i . Note that, $n = 1$ when direct transmission is used, and $n = 2$ when cooperative transmission is used.

C. ACN Outage Probability Expressions

In the following, we will express the probabilities related to $\mathcal{O}_{\text{ACN}}(D_1)$ and $\mathcal{O}_{\text{ACN}}(D_2)$. The outage probability expressions related to D_1 and D_2 , denoted $\mathbb{P}[\mathcal{O}_{\text{ACN}}(D_1)]$ and $\mathbb{P}[\mathcal{O}_{\text{ACN}}(D_2)]$, are respectively given by

$$\mathbb{P}[\mathcal{O}_{\text{ACN}}(D_1)] = 1 - \left[\mathcal{W}_{(D_1)}\left(\frac{\mathcal{G}_1^{(1)}}{I_{SD_1}}\right) + \left\{ \left(1 - \mathcal{W}_{(D_1)}\left(\frac{\mathcal{G}_1^{(1)}}{I_{SD_1}}\right)\right) \times \mathcal{W}_{(D_2)}\left(\frac{\mathcal{G}_1^{(2)}}{I_{SD_2}}\right) \times \mathcal{W}_{(D_1)}\left(\frac{\Theta_1^{(2)}}{I_{D_2D_1}}\right) \right\} \right], \quad (16)$$

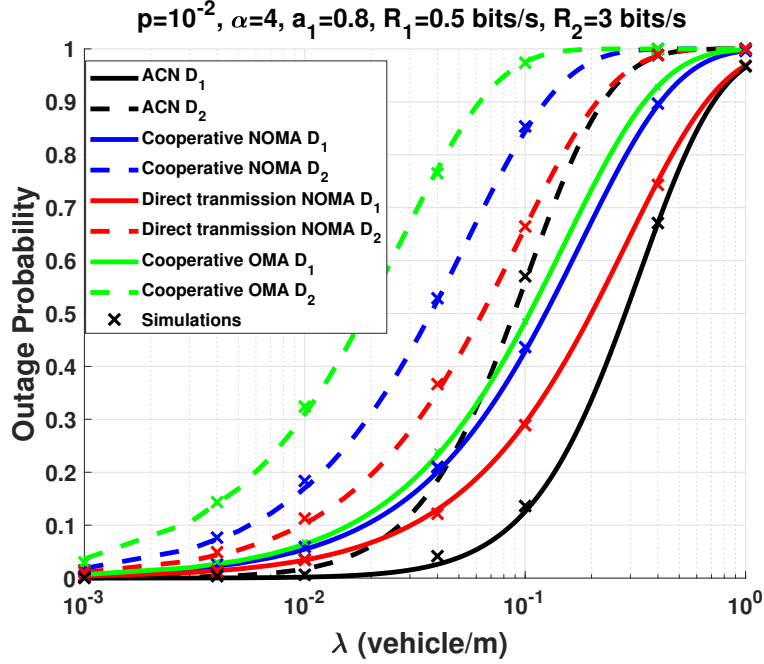


Fig. 4: Outage probability as a function of λ considering ACN, cooperative NOMA, direct transmission NOMA, and cooperative OMA.

and

$$\mathbb{P}\left[\mathcal{O}_{\text{ACN}}(D_2)\right] = 1 - \left[\mathcal{W}_{(D_2)}\left(\frac{\mathcal{G}_{\max}^{(1)}}{I_{SD_2}}\right) + \left\{ \left(1 - \mathcal{W}_{(D_2)}\left(\frac{\mathcal{G}_{\max}^{(1)}}{I_{SD_2}}\right)\right) \times \mathcal{W}_{(D_1)}\left(\frac{\mathcal{G}_{\max}^{(2)}}{I_{SD_1}}\right) \times \mathcal{W}_{(D_2)}\left(\frac{\Theta_2^{(2)}}{I_{D_1D_2}}\right) \right\} \right], \quad (17)$$

where the function $\mathcal{W}_{(D_i)}\left(\frac{A}{B}\right)$ is given by

$$\mathcal{W}_{(D_i)}\left(\frac{A}{B}\right) = \mathcal{L}_{I_{X_{D_i}}}\left(\frac{A}{B}\right) \mathcal{L}_{I_{Y_{D_i}}}\left(\frac{A}{B}\right), \quad (18)$$

and $\mathcal{G}_1^{(n)}$ and $\mathcal{G}_{\max}^{(n)}$, are respectively given by

$$\mathcal{G}_1^{(n)} = \frac{\Theta_1^{(n)}}{a_1 - \Theta_1^{(n)} a_2}, \quad (19)$$

and

$$\mathcal{G}_{\max}^{(n)} = \max(\mathcal{G}_1^{(n)}, \mathcal{G}_2^{(n)}), \quad (20)$$

where $\mathcal{G}_2^{(n)} = \Theta_2^{(n)} / a_2$.

Proof: See Appendix A. ■

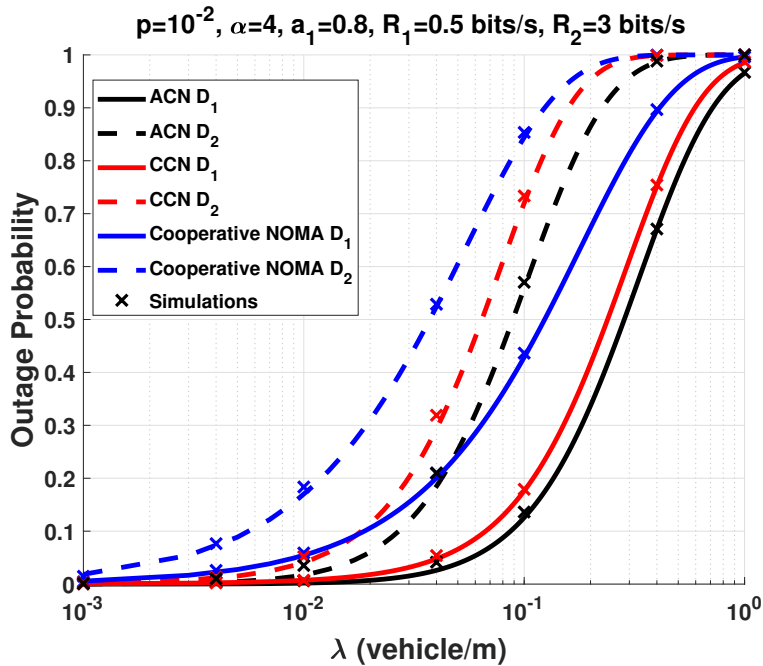


Fig. 5: Outage probability as a function of λ considering ACN, CCN, and cooperative NOMA.

The Laplace transform expressions, $\mathcal{L}_{I_{X_{D_i}}}$ and $\mathcal{L}_{I_{Y_{D_i}}}$, are respectively given by

$$\mathcal{L}_{I_{X_{D_i}}}(s) = \exp\left(\frac{-s p \lambda_X \pi}{\sqrt{s + d_i^2 \sin(\theta_{D_i})^2}}\right), \quad (21)$$

and

$$\mathcal{L}_{I_{Y_{D_i}}}(s) = \exp\left(\frac{-s p \lambda_Y \pi}{\sqrt{s + d_i^2 \cos(\theta_{D_i})^2}}\right). \quad (22)$$

Proof: See Appendix C in [3]. ■

V. SIMULATIONS AND DISCUSSIONS

In this section, we evaluate the performance of NOMA at road intersections. To verify the accuracy of our theoretical analysis, Monte Carlo simulations are performed by averaging over 50,000 realizations of PPPs and fading channel parameters. In all figures, the marks represent the Monte Carlo simulations⁵. We set, without loss of generality, $\lambda_X = \lambda_Y = \lambda$.

⁵The confidence intervals in the simulations are very small, this is why they have been omitted.

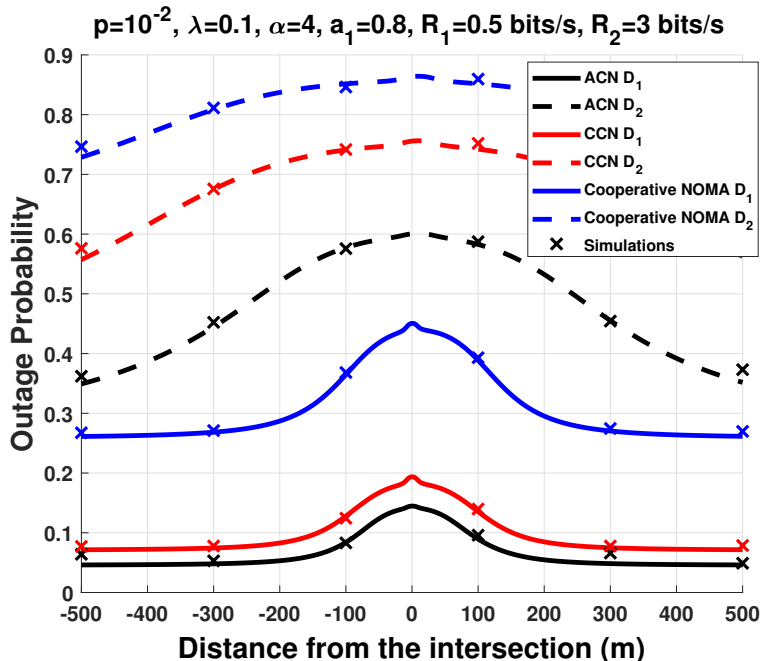


Fig. 6: Outage probability as a function of the distance from the intersection, considering ACN, CCN, and cooperative NOMA.

Fig.4 shows the outage probability as a function of λ considering ACN, cooperative transmission using NOMA [3], direct transmission using NOMA [28], and the classical cooperative OMA. We can see from Fig.4, that as the intensity of vehicles λ increases, the outage probability increases. This is because as the intensity increases, the number of interfering vehicles increases, which decreases the SIR at the receiving node. We can also see from Fig.4, that the ACN protocol outperforms the cooperative transmission using NOMA, direct transmission using NOMA, and the classical cooperative OMA. This is because, the ACN protocol can switch its transmission scheme. Hence, it uses the direct transmission in the first phase, when it fails, it switch to the cooperative transmission in the second phase.

Fig.5 shows the outage probability as a function of λ considering ACN, CCN [21], and cooperative NOMA. We can see from Fig.5, that both ACN and CCN outperform the cooperative transmission using NOMA. We can also see that ACN outperforms CCN for both D_1 and D_2 . This is because the transmission in CCN occurs in two phases, hence it reduces its spectral efficiency. On the other hand, the ACN protocol occurs in one phase if the direct transmission succeed, which increases the spectral efficiency compared to CCN. Also, during the second phase of the cooperative transmission, the ACN use OMA to transmit the message since there is only

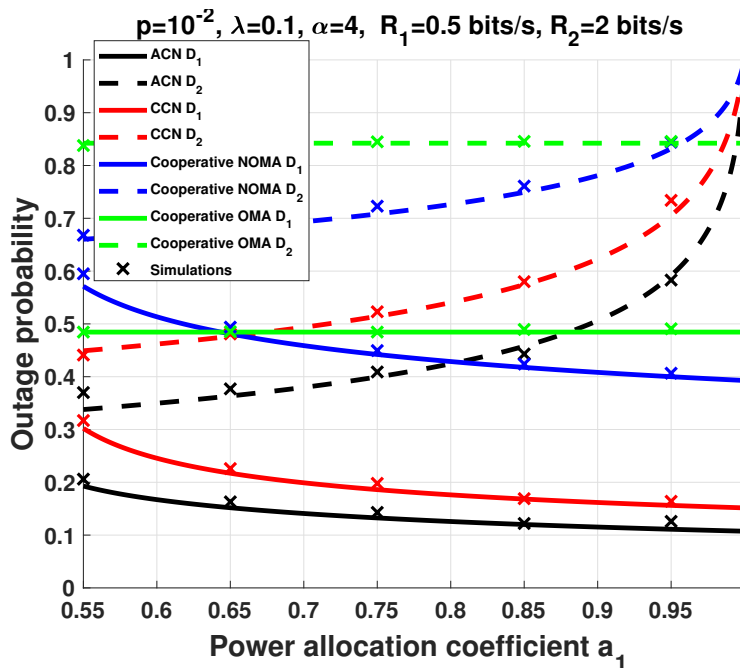


Fig. 7: Outage probability as a function of the power allocation coefficient a_1 , considering ACN, CCN, cooperative NOMA, and cooperative OMA.

one signal to transmit in the second hop ($D_1 \rightarrow D_2$ or $D_2 \rightarrow D_1$). Hence, it increases the SIR at the receiver node.

Fig.6 plots the outage probability as a function of the nodes distance from the intersection, considering ACN, CCN, and cooperative NOMA. We assume that the distance between S , D_1 , and D_2 does not change through the simulation. Hence, the nodes of triplet $\{S, D_1, D_2\}$ move together towards the intersection. We set $\|S - D_1\| = \|S - D_2\| = 100$ m. We can see from Fig.6, that as the nodes come closer to the intersection (200 m for D_1 and 500 m for D_2), the outage probability increases. This is because, when the nodes are at the intersection, the interfering vehicles from the X road and the Y road both contribute to the aggregate interference, which decreases the SIR at the receiving nodes. We can also see that, ACN outperforms both CCN and cooperative NOMA at the intersection. However, we can see that there is a big gap in performance between ACN and CCN regarding D_2 . This is because, the spectral efficiency of CCN decrease drastically for high data rates. This is why, ACN protocol offers a better performance for high data rates compared to CCN. Finally, we can see in CCN and cooperative NOMA, that the outage probability increases more in the last 10 m. However, there is no increases in the outage probability when using ACN.

Fig.7 plots the outage probability as a function of a_1 , considering ACN, CCN, cooperative NOMA, and cooperative OMA. We can see from Fig.7, that ACN outperforms CCN and cooperative NOMA and cooperative OMA regardless of a_1 value. We can also see that when a_1 increases, the outage probability of D_1 decreases, whereas the outage probability of D_2 increases. Finally, we can see that the performance of ACN is greater for D_2 , since D_2 has a high data rate.

VI. CONCLUSION

In this paper, we proposed and evaluated the performance of ACN protocol at road intersections. We calculated the outage probability related to ACN protocol, and closed form expressions were obtained for two destination nodes. We compared the ACN protocol with cooperative NOMA protocol, direct NOMA protocol, and the classical cooperative OMA protocol, and we showed that ACN protocol outperforms these protocols in terms of outage probability, especially at intersections. We also compared the performance of ACN protocol with the CCN protocol, and we showed that the ACN protocol offers better performance than CCN protocol at road intersections in terms of outage probability. Finally, we showed that the performance of ACN protocol increases compared to other existing protocols for high data rates.

APPENDIX A

The probability $\mathbb{P}\left[\mathcal{O}_{\text{ACN}}(D_1)\right]$ is expressed as

$$\mathbb{P}\left[\mathcal{O}_{\text{ACN}}(D_1)\right] = 1 - \mathbb{P}\left[\mathcal{O}_{\text{ACN}}^{\text{C}}(D_1)\right]. \quad (23)$$

The probability $\mathbb{P}\left[\mathcal{O}_{\text{ACN}}^{\text{C}}(D_1)\right]$ is given by

$$\mathbb{P}\left[\mathcal{O}_{\text{ACN}}^{\text{C}}(D_1)\right] = \mathbb{P}\left(\text{DT}_{SD_1}^{\text{C}}\right) + \left\{ \mathbb{P}\left(\text{DT}_{SD_1}\right) \times \mathbb{P}\left(\text{RT}_{S,D_2,D_1}^{\text{C}}\right) \right\}. \quad (24)$$

To calculate $\mathbb{P}\left(\text{DT}_{SD_1}^{\text{C}}\right)$, we proceed as follows

$$\mathbb{P}\left(\text{DT}_{SD_1}^{\text{C}}\right) = \mathbb{P}\left(\text{SIR}_{SD_{1-1}} \geq \Theta_1^{(1)}\right) \quad (25)$$

plugging (3) into (25), we get

$$\begin{aligned} \mathbb{P}\left(\text{DT}_{SD_1}^{\text{C}}\right) &= \mathbb{E}_{I_X, I_Y} \left[\mathbb{P} \left\{ \frac{|h_{SD_1}|^2 l_{SD_1} a_1}{|h_{SD_1}|^2 l_{SD_1} a_2 + I_{X_{D_1}} + I_{Y_{D_1}}} \geq \Theta_1^{(1)} \right\} \right] \\ &= \mathbb{E}_{I_X, I_Y} \left[\mathbb{P} \left\{ |h_{SD_1}|^2 l_{SD_1} (a_1 - \Theta_1^{(1)} a_2) \geq \Theta_1^{(1)} [I_{X_{D_1}} + I_{Y_{D_1}}] \right\} \right]. \end{aligned} \quad (26)$$

We can see from (26) that, when $\Theta_1^{(1)} \geq a_1/a_2$, the success probability $\mathbb{P}\left(\text{DT}_{SD_1}^C\right) = 0$. Then, when $\Theta_1^{(1)} < a_1/a_2$, and after setting $\mathcal{G}_1^{(1)} = \Theta_1^{(1)}/(a_1 - \Theta_1^{(1)}a_2)$, we get

$$\mathbb{P}\left(\text{DT}_{SD_1}^C\right) = \mathbb{E}_{I_X, I_Y} \left[\mathbb{P} \left\{ |h_{SD_1}|^2 \geq \frac{\mathcal{G}_1^{(1)}}{l_{SD_1}} [I_{X_{D_1}} + I_{Y_{D_1}}] \right\} \right].$$

Since $|h_{SD_1}|^2$ follows an exponential distribution with unit mean, and using the independence of the PPP on the road X and Y , we obtain

$$\mathbb{P}\left(\text{DT}_{SD_1}^C\right) = \mathbb{E}_{I_X} \left[\exp \left(-\frac{\mathcal{G}_1^{(1)}}{l_{SD_1}} I_{X_{D_1}} \right) \right] \mathbb{E}_{I_Y} \left[\exp \left(-\frac{\mathcal{G}_1^{(1)}}{l_{SD_1}} I_{Y_{D_1}} \right) \right].$$

Given that $\mathbb{E}[e^{sI}] = \mathcal{L}_I(s)$, we finally get

$$\mathbb{P}\left(\text{DT}_{SD_1}^C\right) = \mathcal{L}_{I_{X_{D_1}}}\left(\frac{\mathcal{G}_1^{(1)}}{l_{SD_1}}\right) \mathcal{L}_{I_{Y_{D_1}}}\left(\frac{\mathcal{G}_1^{(1)}}{l_{SD_1}}\right). \quad (27)$$

Following the same steps, we obtain

$$\mathbb{P}\left(\text{DT}_{SD_1}\right) = 1 - \mathcal{L}_{I_{X_{D_1}}}\left(\frac{\mathcal{G}_1^{(1)}}{l_{SD_1}}\right) \mathcal{L}_{I_{Y_{D_1}}}\left(\frac{\mathcal{G}_1^{(1)}}{l_{SD_1}}\right). \quad (28)$$

To calculate $\mathbb{P}\left(\text{RT}_{S, D_2, D_1}^C\right)$, we proceed as follows

$$\mathbb{P}\left(\text{RT}_{S, D_2, D_1}^C\right) = \mathbb{P}\left(\text{SIR}_{SD_{2-1}} \geq \Theta_1^{(2)}\right) \times \mathbb{P}\left(\text{SIR}_{D_2, D_1}^{(\text{OMA})} \geq \Theta_1^{(2)}\right). \quad (29)$$

The probability $\mathbb{P}\left(\text{SIR}_{SD_{2-1}} \geq \Theta_1^{(2)}\right)$ can be acquired following the same steps above, and it is given by

$$\mathbb{P}\left(\text{SIR}_{SD_{2-1}} \geq \Theta_1^{(2)}\right) = \mathcal{L}_{I_{X_{D_2}}}\left(\frac{\mathcal{G}_1^{(2)}}{l_{SD_2}}\right) \mathcal{L}_{I_{Y_{D_2}}}\left(\frac{\mathcal{G}_1^{(2)}}{l_{SD_2}}\right). \quad (30)$$

The probability $\mathbb{P}\left(\text{SIR}_{D_2, D_1}^{(\text{OMA})} \geq \Theta_1^{(2)}\right)$ can be easily calculated, and it is given by

$$\mathbb{P}\left(\text{SIR}_{D_2, D_1}^{(\text{OMA})} \geq \Theta_1^{(2)}\right) = \mathcal{L}_{I_{X_{D_1}}}\left(\frac{\Theta_1^{(2)}}{l_{D_2, D_1}}\right) \mathcal{L}_{I_{Y_{D_1}}}\left(\frac{\Theta_1^{(2)}}{l_{D_2, D_1}}\right). \quad (31)$$

In the same way, we express The probability $\mathbb{P}\left[\mathcal{O}_{\text{ACN}}(D_2)\right]$ as a function of a success probability $\mathbb{P}\left[\mathcal{O}_{\text{ACN}}^C(D_2)\right]$ as follows

$$\mathbb{P}\left[\mathcal{O}_{\text{ACN}}(D_2)\right] = 1 - \mathbb{P}\left[\mathcal{O}_{\text{ACN}}^C(D_2)\right]. \quad (32)$$

The probability $\mathbb{P}\left[\mathcal{O}_{\text{ACN}}^C(D_2)\right]$ is given by

$$\mathbb{P}\left[\mathcal{O}_{\text{ACN}}^C(D_2)\right] = \mathbb{P}\left(\text{DT}_{SD_2}^C\right) + \left\{ \mathbb{P}\left(\text{DT}_{SD_2}\right) \times \mathbb{P}\left(\text{RT}_{S, D_1, D_2}^C\right) \right\}. \quad (33)$$

To calculate $\mathbb{P}\left(\text{DT}_{SD_2}^C\right)$, we proceed as follows

$$\begin{aligned}\mathbb{P}\left(\text{DT}_{SD_2}^C\right) &= \mathbb{P}\left(\bigcap_{i=1}^2 \text{SIR}_{SD_{2-i}} \geq \Theta_i^{(1)}\right) \\ &= \mathbb{P}\left(\text{SIR}_{SD_{2-1}} \geq \Theta_1^{(1)} \cap \text{SIR}_{SD_{2-2}} \geq \Theta_2^{(1)}\right).\end{aligned}\quad (34)$$

Following the same steps as for $\mathbb{P}\left(\text{DT}_{SD_1}^C\right)$, we get

$$\mathbb{P}\left(\text{DT}_{SD_2}^C\right) = \mathbb{E}_{I_X, I_Y} \left[\mathbb{P} \left\{ \frac{|h_{SD_2}|^2 l_{SD_2} a_1}{|h_{SD_2}|^2 l_{SD_2} a_2 + I_{X_{D_2}} + I_{Y_{D_2}}} \geq \Theta_1^{(1)}, \frac{|h_{SD_2}|^2 l_{SD_2} a_2}{I_{X_{D_2}} + I_{Y_{D_2}}} \geq \Theta_2^{(1)} \right\}, \right]$$

When $\Theta_1^{(1)} > a_1/a_2$, then $\mathbb{P}\left(\text{DT}_{SD_2}^C\right) = 0$, otherwise we continue the derivation. We set $\mathcal{G}_2^{(1)} = \Theta_2^{(1)}/a_2$, then

$$\mathbb{P}\left(\text{DT}_{SD_2}^C\right) = \mathbb{E}_{I_X, I_Y} \left[\mathbb{P} \left\{ |h_{SD_2}|^2 \geq \frac{\mathcal{G}_1^{(1)}}{l_{SD_2}} [I_{X_{D_2}} + I_{Y_{D_2}}], |h_{SD_2}|^2 \geq \frac{\mathcal{G}_2^{(1)}}{l_{SD_2}} [I_{X_{D_2}} + I_{Y_{D_2}}] \right\} \right].$$

Finally, $\mathbb{P}\left(\text{DT}_{SD_2}^C\right)$ equals

$$\mathbb{P}\left(\text{DT}_{SD_2}^C\right) = \mathcal{L}_{I_{X_{D_2}}} \left(\frac{\mathcal{G}_{\max}^{(1)}}{l_{SD_2}} \right) \mathcal{L}_{I_{Y_{D_2}}} \left(\frac{\mathcal{G}_{\max}^{(1)}}{l_{SD_2}} \right), \quad (35)$$

where $\mathcal{G}_{\max}^{(1)} = \max(\mathcal{G}_1^{(1)}, \mathcal{G}_2^{(1)})$.

To calculate $\mathbb{P}\left(\text{RT}_{S,D_1,D_2}^C\right)$, we follow the same steps as in $\mathbb{P}\left(\text{RT}_{S,D_2,D_1}^C\right)$.

REFERENCES

- [1] U.S. Dept. of Transportation, National Highway Traffic Safety Administration, “Traffic safety facts 2015,” Jan. 2017.
- [2] Z. Ding, Z. Yang, P. Fan, and H. V. Poor, “On the performance of non-orthogonal multiple access in 5g systems with randomly deployed users,” *IEEE Signal Processing Letters*, vol. 21, no. 12, pp. 1501–1505, 2014.
- [3] B. E. Y. Belmekki, A. Hamza, and B. Escrig, “On the outage probability of cooperative 5g noma at intersections,” in *2019 IEEE 89th Vehicular Technology Conference (VTC2019-Spring)*, pp. 1–6, IEEE, 2019.
- [4] M. J. Farooq, H. ElSawy, and M.-S. Alouini, “A stochastic geometry model for multi-hop highway vehicular communication,” *IEEE Transactions on Wireless Communications*, vol. 15, no. 3, pp. 2276–2291, 2016.
- [5] Z. Tong, H. Lu, M. Haenggi, and C. Poellabauer, “A stochastic geometry approach to the modeling of dsrc for vehicular safety communication,” *IEEE Transactions on Intelligent Transportation Systems*, vol. 17, no. 5, pp. 1448–1458, 2016.
- [6] C. Jiang, H. Zhang, Z. Han, Y. Ren, V. C. Leung, and L. Hanzo, “Information-sharing outage-probability analysis of vehicular networks,” *IEEE Transactions on Vehicular Technology*, vol. 65, no. 12, pp. 9479–9492, 2016.
- [7] E. Steinmetz, M. Wildemeersch, T. Q. Quek, and H. Wymeersch, “A stochastic geometry model for vehicular communication near intersections,” in *Globecom Workshops (GC Wkshps), 2015 IEEE*, pp. 1–6, IEEE, 2015.
- [8] M. Abdulla, E. Steinmetz, and H. Wymeersch, “Vehicle-to-vehicle communications with urban intersection path loss models,” in *Globecom Workshops (GC Wkshps), 2016 IEEE*, pp. 1–6, IEEE, 2016.

- [9] J. P. Jeyaraj and M. Haenggi, "Reliability analysis of v2v communications on orthogonal street systems," in *GLOBECOM 2017-2017 IEEE Global Communications Conference*, pp. 1–6, IEEE, 2017.
- [10] Z. Zhang, H. Sun, R. Q. Hu, and Y. Qian, "Stochastic geometry based performance study on 5g non-orthogonal multiple access scheme," in *Global Communications Conference (GLOBECOM), 2016 IEEE*, pp. 1–6, IEEE, 2016.
- [11] Z. Zhang and R. Q. Hu, "Uplink non-orthogonal multiple access with fractional power control," in *Wireless Communications and Networking Conference (WCNC), 2017 IEEE*, pp. 1–6, IEEE, 2017.
- [12] Z. Zhang, H. Sun, and R. Q. Hu, "Downlink and uplink non-orthogonal multiple access in a dense wireless network," *IEEE Journal on Selected Areas in Communications*, vol. 35, no. 12, pp. 2771–2784, 2017.
- [13] B. E. Y. Belmekki, A. Hamza, and B. Escrig, "On the performance of 5g non-orthogonal multiple access for vehicular communications at road intersections," *Vehicular Communications*, p. doi:10.1016/j.vehcom.2019.100202, 2019.
- [14] B. E. Y. Belmekki, A. Hamza, and B. Escrig, "Performance analysis of cooperative noma at intersections for vehicular communications in the presence of interference," *Ad hoc Networks*, p. doi:10.1016/j.adhoc.2019.102036, 2019.
- [15] B. E. Y. Belmekki, A. Hamza, and B. Escrig, "Outage analysis of cooperative noma using maximum ratio combining at intersections," in *2019 wireless and mobile computing, networking and communications (WiMob 2019), Barcelona, Spain*, pp. 1–6, 2019.
- [16] B. E. Y. Belmekki, A. Hamza, and B. Escrig, "Non-orthogonal multiple access performance for millimeter wave in vehicular communications," *arXiv preprint arXiv:1909.12392*, 2019.
- [17] B. E. Y. Belmekki, A. Hamza, and B. Escrig, "Outage analysis of cooperative noma in millimeter wave vehicular network at intersections," *arXiv preprint arXiv:1904.11022*, 2019.
- [18] B. E. Y. Belmekki, A. Hamza, and B. Escrig, "Performance analysis of cooperative communications at road intersections using stochastic geometry tools," *arXiv preprint arXiv:1807.08532*, 2018.
- [19] B. E. Y. Belmekki, A. Hamza, and B. Escrig, "Cooperative vehicular communications at intersections over nakagami-m fading channels," *Vehicular Communications*, p. doi:10.1016/j.vehcom.2019.100165, 07 2019.
- [20] B. E. Y. Belmekki, A. Hamza, and B. Escrig, "On the outage probability of vehicular communications at intersections over nakagami-m fading channels," *arXiv preprint arXiv:1912.05325*, 2019.
- [21] Z. Ding, M. Peng, and H. V. Poor, "Cooperative non-orthogonal multiple access in 5g systems," *IEEE Communications Letters*, vol. 19, no. 8, pp. 1462–1465, 2015.
- [22] Y. Hu, M. C. Gursoy, and A. Schmeink, "Efficient transmission schemes for low-latency networks: Noma vs. relaying," in *2017 IEEE 28th Annual International Symposium on Personal, Indoor, and Mobile Radio Communications (PIMRC)*, pp. 1–6, IEEE, 2017.
- [23] T. V. Nguyen, F. Baccelli, K. Zhu, S. Subramanian, and X. Wu, "A performance analysis of csma based broadcast protocol in vanets," in *2013 Proceedings IEEE INFOCOM*, pp. 2805–2813, IEEE, 2013.
- [24] Z. Ding, H. Dai, and H. V. Poor, "Relay selection for cooperative noma," *IEEE Wireless Communications Letters*, vol. 5, no. 4, pp. 416–419, 2016.
- [25] Z. Ding, L. Dai, and H. V. Poor, "Mimo-noma design for small packet transmission in the internet of things," *IEEE access*, vol. 4, pp. 1393–1405, 2016.
- [26] B. E. Y. Belmekki, A. Hamza, and B. Escrig, "Outage performance of NOMA at road intersections using stochastic geometry," in *2019 IEEE Wireless Communications and Networking Conference (WCNC) (IEEE WCNC 2019)*, pp. 1–6, IEEE, 2019.
- [27] M. O. Hasna, M.-S. Alouini, A. Bastami, and E. S. Ebbini, "Performance analysis of cellular mobile systems with successive co-channel interference cancellation," *IEEE Transactions on Wireless Communications*, vol. 2, no. 1, pp. 29–40, 2003.

- [28] B. E. Y. Belmekki, A. Hamza, and B. Escrig, "Outage performance of NOMA at road intersections using stochastic geometry," in *2019 IEEE Wireless Communications and Networking Conference (WCNC) (IEEE WCNC 2019)*, (Marrakech, Morocco), Apr. 2019.